Available online at www.sciencedirect.com
SCIENCE DIRECT®
Journal of Nuclear Materials 345 (2005) 219–224
journal of nuclear materials
www.elsevier.com/locate/jnucmat

Dynamics for oxidation of Fe_3O_4, Fe_2CoO_4 and Fe_2NiO_4

Maryam Abili Nejad, Mats Jonsson *

Department of Chemistry, Nuclear Chemistry, Royal Institute of Technology, SE-100 44 Stockholm, Sweden

Received 4 November 2004; accepted 7 June 2005

Abstract

The kinetics for oxidation of CRUD model compounds (Fe_3O_4, Fe_2CoO_4, and Fe_2NiO_4) by $IrCl_6^{2-}$ and MnO_4^- has been studied using aqueous suspensions of metal oxide powder. The second order rate constants at room temperature were determined to $3.6(\pm0.3)\times10^{-6}$, $1.2(\pm0.2)\times10^{-5}$ and $3.3(\pm0.5)\times10^{-6}$ min^{-1} m for Fe_3O_4, Fe_2CoO_4 and Fe_2NiO_4 reacting with $IrCl_6^{-2}$ and to $1.5(\pm0.2)\times10^{-6}$, $1.2(\pm0.1)\times10^{-6}$ and $6(\pm1)\times10^{-7}$ min^{-1} m for the reactions with MnO_4^-. The reactivity of the metal oxides is in the order $Fe_2CoO_4 > Fe_3O_4 > Fe_2NiO_4$ for both oxidants. Unlike previous studies on oxidation of UO_2, there is no linear relation between the logarithm of the rate constant, $\ln k$, and the one-electron reduction potential of the oxidants for the metal oxides studied here. This discrepancy is explained in terms of differences in the reorganization energy of the metal oxides giving rise to different curvature in accordance with the Marcus theory for electron transfer.

1. Introduction

Corrosion products released from out-of-core metal surfaces of nuclear power plants are mobilised and can be transferred to the core by the coolant. In the core they deposit on the fuel surfaces to build up fuel CRUD (Chalk River Unidentified Deposit, mostly containing Fe_2O_3, Fe_3O_4, Fe_2CoO_4, and Fe_2NiO_4) [1,2]. Due to the intense flux of neutrons in the core, the corrosion products become highly activated. Corrosion products can then be released from the fuel surfaces and subsequently be transported to other parts of the systems where they can be deposited on the surfaces of the cooling loop pipes. Power plant personnel may thus be exposed to increased levels of ionizing radiation. There is also a risk of release of radionuclides from the cooling circuits following some coolant loop failure.

Metal oxides have low reactivity in water under normal conditions. It should be noted that magnetite has thermodynamically a very high solubility at room temperature under reducing conditions and that it is not thermodynamically stable under oxidizing conditions. However, kinetic restrictions limit the actual solubility [3]. Radiolysis of water produces strong oxidants and reductants. Therefore, studying the reactivity of oxidants with CRUD components is motivated. In addition, the presence of reactive metal oxide surfaces can significantly affect the concentration of oxidants and reductants in the reactor.

To the best of our knowledge there are very few publications on the mechanism and reactivity of the metal oxides Fe_3O_4, Fe_2CoO_4, and Fe_2NiO_4 (the major components of CRUD) towards oxidants in aqueous solutions. Feitknecht et al. concluded that the final solid product of oxidation of Fe_3O_4 depends on the particle

* Corresponding author. Tel.: +46 8 7909123; fax: +46 8 7908772.
E-mail address: matsj@nuchem.kth.se (M. Jonsson).

0022-3115/$ - see front matter © 2005 Elsevier B.V. All rights reserved.
doi:10.1016/j.jnucmat.2005.06.001

size of Fe_3O_4 [4]. The mechanism proposed was based on the diffusion of iron cations, for small and large particles (sub microns) the end products are α-Fe_2O_3 and γ-Fe_2O_3 respectively. They also postulated that particle size has effect on the rate of the reactions. However, Colombo et al. [5] criticized this work and showed that below 400 °C pure magnetite never oxidize to α-Fe_2O_3 and that particle size only affects the kinetics of the reaction. Sidhu et al. have studied the oxidation mechanism of magnetite, Fe_2CoO_4, Fe_2NiO_4 and Fe_2ZnO_4 in the temperature range of 170–200 °C [6]. They developed a theory on the basis of diffusion theory and concluded that during oxidation of magnetite the surface area of magnetite did not change and therefore the size of the particles was not altered. They also suggested that it is the iron ion, which is diffusing out of the crystals of magnetite during the oxidation process.

Jolivet and Tronc showed that in acid media magnetite crystals are oxidized to γ-Fe_2O_3 by an adsorption reaction which traps mobile electrons from the bulk material and reduces the interfacial Fe^{III} [7]. Zheng-Ya and Muir [8] investigated the relative rates of dissolution of copper, zinc, and nickel ferrites and magnetite in HCl solutions under oxidizing and reducing conditions. An analogous system (oxidation of metal oxide) is oxidation of UO_2. Several studies on the kinetics of UO_2 oxidation have been performed. Recently, a linear relationship between the one-electron reduction potential for the oxidant, H_2O_2, MnO_4^-, $IrCl_6^{2-}$ and $Fe(EDTA)^-$ and the logarithm of the rate constant for oxidation of UO_2 has been observed [9].

Recently, we have studied the trend in reactivity of the metal oxides (Fe_3O_4, Fe_2CoO_4, and Fe_2NiO_4) with H_2O_2 [10], the latter being one of the products formed upon radiolysis of water. ICP measurements of the solution after reaction between H_2O_2 and the metal oxides indicate that the main final solid oxidation product for all three CRUD model compounds is Fe_2O_3. This is well in line with previous studies reporting γ-Fe_2O_3 (maghemite) to be formed upon oxidation of Fe_3O_4 [4]. The trend in reactivity was shown to be $Fe_2CoO_4 > Fe_3O_4 > Fe_2NiO_4$. This trend is somewhat unexpected from a thermodynamical point of view (the expected trend is $Fe_3O_4 > Fe_2CoO_4 > Fe_2NiO_4$) but can probably be attributed to the difference in particle size between the three metal oxide powders used in the experiment. Both the pre-exponential factor in the Arrhenius equation and the activation energy were shown to strongly depend on the particle size. In order to obtain more general information concerning the relationship between the nature of the oxidant (i.e. reduction potential) and the rate constant for metal oxide oxidation we have investigated the oxidation of Fe_3O_4, Fe_2CoO_4, and Fe_2NiO_4 using two more potent oxidants, $IrCl_6^{2-}$ and MnO_4^-. The purpose of this was to find relationships useful for estimation of the reactivity of unstable radiolytic oxidants (e.g. $OH^{\cdot}$ and $HO_2^{\bullet}$ towards CRUD.

2. Experimental

The chemicals used throughout this study were of analytical grade or purer and were obtained from commercial sources as Aldrich, Merck, BDH and AGA. The metal oxides (Fe_3O_4, Fe_2CoO_4, and Fe_2NiO_4) were obtained from KEBO and Alfa Aesar. The oxidants used are $IrCl_6^{2-}$ and MnO_4^-. The water was Millipore purified prior to use.

The metal oxide powders were pre-washed in two steps, first with 0.1 M EDTA and then with pure water [10]. The specific surface areas of the three metal oxides, Fe_3O_4, Fe_2CoO_4 and Fe_2NiO_4 were determined by BET measurement to be 6.59, 1.05 and 2.12 m^2/g, respectively, using a Flowsorb 2300II. The measurement was performed at room temperature. The gas used in this method was a mixture of N_2 30% and He 70%. UV–vis spectroscopy was used to analyse the oxidant concentration of the samples, using a Jasco V-530 UV–vis spectrophotometer.

The initial concentrations of Sodium hexachloroirridate (IV) hexahydrate and potassium permanganate used in these experiments were determined to 0.1 mM. Varied amounts of the three solid metal oxides, 0.2–2.0 g were added to the $IrCl_6^{2-}$ and MnO_4^- solutions to obtain 18 ml suspension volume. The solutions were purged with Ar for 20 min prior to addition of the metal oxide powder and throughout the experiments for mixing purpose and to keep the concentration of oxygen as low as possible.

Before each analysis, the sample solution was filtered to stop the reaction and to clear the solution. Sampling and filtration normally takes less than 10 s. The time to perform an experiment varied from approximately 10 min to more than one hour depending on tempera-

Table 1
Experimental conditions

Oxidant	Initial conc. (mM)	E^0 (V vs NHE)	Wavelength (nm)	Volume (ml)
$IrCl_6^{2-}$	0.1	0.8665 [17]	488	18
MnO_4^-	0.1	0.576 [17]	525	18
H_2O_2 [10]	4.5	0.46 [18]	360	18

ture, oxidant and amount of metal oxide. The pore size of the filter is 0.2 μm. The absorption of the oxidants, $IrCl_6^{-2}$ and MnO_4^- was then measured by UV–vis spectrometer. $IrCl_6^{2-}$ absorbs at 488 nm and MnO_4^- absorbs at 525 nm. The reaction between MnO_4^- and Fe_3O_4 was studied in the temperature range 25–80 °C in order to determine the activation energy. All other experiments were performed at room temperature.

The experimental conditions are summarized in Table 1. The experimental conditions for the recently published H_2O_2 experiments [10] are also included in the table since the results from these experiments are important for the discussion in this paper.

3. Results and discussion

The characteristics of the metal oxide powders used in this work are summarized in Table 2.

The approximate particle radii were estimated from the specific surface area (determined by BET) and the density of the materials. It should be noted that the particles of a given powder are not uniform in size. The estimated particle radii are merely describing the average size.

It is evident that both oxidants used in this study are capable of oxidizing all three metal oxides at appreciable rates also at room temperature. This was not the case for H_2O_2 which showed no reactivity towards Fe_2NiO_4 at room temperature. However, the rate constant for this reaction at room temperature was estimated from the Arrhenius equation. The reactions between MnO_4^- and $IrCl_6^{2-}$ and the three metal oxides are first order processes (exemplified for MnO_4^- in Fig. 1).

By repeating experiments at various solid surface to solution volume ratios it is possible to determine the second order rate constant for the process. The second order rate constants for the reactions between the oxidants and the metal oxide powders were determined from slope obtained when plotting the observed pseudo first order rate constants against the surface to volume ratio (Fig. 2).

The resulting second order rate constants (based on oxidant concentration and surface area) are summarized in Table 3 along with previously published data for the reaction between H_2O_2 and the three metal oxides studied in this work. For comparison, the corresponding data for oxidation of UO_2 is also included.

Table 2
Characteristics of metal oxide powders

Metal oxides	Specific surface area (m^2/g)	Radius (μm)	ZPC (pH)
Fe_3O_4	6.59	91	7 [19,20]
$CoFe_2O_4$	1.05	571	6.5 [20,21]
$NiFe_2O_4$	2.12	283	6.7 [20,22]
UO_2	5.85	47	5–5.5 [23]

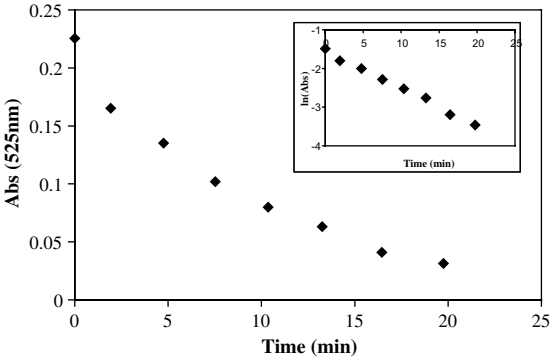

Fig. 1. MnO_4^- absorbance (at 525 nm) as a function of reaction time at 25 °C (with 2 g Fe_2NiO_4).

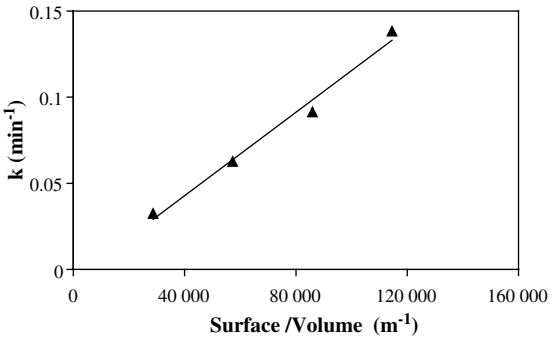

Fig. 2. Pseudo first order rate constants plotted against surface/volume ratio at 25 °C for the reaction between Fe_2CoO_4 and MnO_4^-.

As can be seen, $IrCl_6^{2-}$ is the most reactive oxidant while H_2O_2 is the least reactive oxidant for all four metal oxides. It is also obvious that Fe_2NiO_4 is the least reactive metal oxide while UO_2 is the most reactive metal oxide. These observations are well in line with what can be expected from the thermodynamics of the different reaction systems. The relative reactivity of Fe_2CoO_4 and Fe_3O_4 is still not in accordance with what we would expect from a thermodynamical point of view. However, the difference in reactivity is fairly small. The difference in particle size between the Fe_3O_4 and Fe_2CoO_4 powders is expected to affect the relative reactivity significantly according to Eq. (1) [10]

$$\frac{d[OX]}{dt} = -\frac{2k_B T}{3\pi\eta}\frac{R_{MOX}^2}{R_{OX}R_p}\left(e^{\frac{-E_a}{RT}}\right)[OX]\frac{N_{MOX}}{V}, \quad (1)$$

where k_B denotes the Boltzmann constant, η is the viscosity and R_{MOX}, R_{OX} and R_p denote the radii for

Table 3
Rate constants for reactions between metal oxides and oxidants

Metal oxide	H_2O_2 (min^{-1} m)	$IrCl_6^{2-}$ (min^{-1} m)[a]	MnO_4^- (min^{-1} m)[a]	$IrCl_6^{2-}$ (pH 4) (min^{-1} m)	MnO_4^- (pH 4) (min^{-1} m)
Fe_3O_4	$6.6\ (\pm0.4)\times10^{-9}$	$3.6\ (\pm0.3)\times10^{-6}$	$1.5\ (\pm0.2)\times10^{-6}$	$1.4\ (\pm0.2)\times10^{-5}$	$3.4\ (\pm0.4)\times10^{-6}$
$CoFe_2O_4$	$3.4\ (\pm0.4)\times10^{-8}$	$1.2\ (\pm0.2)\times10^{-5}$	$1.2\ (\pm0.1)\times10^{-6}$	$2.1\ (\pm0.2)\times10^{-5}$	$3.4\ (\pm0.7)\times\ 10^{-6}$
$NiFe_2O_4$	No reaction	$3.3\ (\pm0.5)\times10^{-6}$	$6\ (\pm1)\times10^{-7}$	$1.4\ (\pm0.2)\times10^{-6}$	$7.9\ (\pm0.7)\times\ 10^{-7}$
UO_2 [9]	8.05×10^{-7}	4.60×10^{-5}	2.72×10^{-6}	–	–

[a] Determined from experiments performed in unbuffered solutions.

molecular metal oxide, the oxidant molecule and the solid particle, respectively.

Furthermore, the activation energy, E_a for oxidation of solid surfaces in particle suspensions appears to decrease with increasing particle size [10]. For these reasons, direct comparison of kinetic results from experiments in different particle suspensions are difficult to perform. Without detailed information on how the activation energy is affected by the particle size, extrapolation of experimental data to other particle sizes than the actual size used in the experiment is impossible. Hence, the rate constants presented in Table 3 must be regarded as system specific.

It was previously shown for oxidation of UO_2 that the logarithm of the rate constant for the reaction is linearly related to the one-electron reduction potential of the oxidant. In Fig. 3 we have plotted $\ln k$ against E^0 for the oxidant for the metal oxides studied in this work and for UO_2.

Clearly, there is no linear relation between $\ln k$ and E^0 for the metal oxides studied here.

To elucidate the discrepancy between UO_2 and the other three metal oxides we employ the Marcus theory for electron transfer [11–13]. According to the Marcus theory the rate constant for electron transfer processes ($A^n + B^m \rightarrow A^{n-1} + B^{m+1}$) in solution is given by Eq. (2)

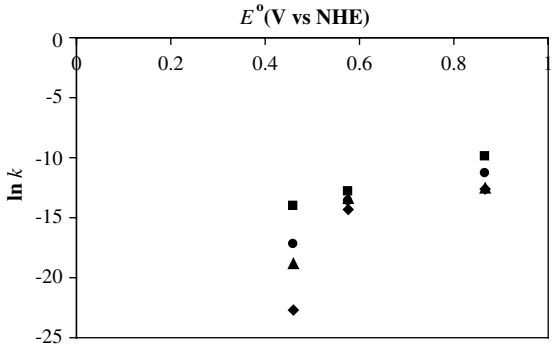

Fig. 3. The logarithm of the second order rate constant, $\ln k$, for oxidation of metal oxides in unbuffered aqueous solution plotted against the one electron reduction potential of the oxidant, E^0 at 25 °C: (■) UO_2; (▲) Fe_3O_4; (●) Fe_2CoO_4; (♦) Fe_2NiO_4.

$$k = Ze^{-\frac{\lambda_{12}}{RT}\left(1+\frac{\Delta G^0}{\lambda_{12}}\right)^2}, \tag{2}$$

where Z is the collision frequency, ΔG^0 is the change in free energy and λ_{12} is the reorganization energy. The reorganization energy for the reaction is derived from the reorganization energies of the corresponding self-exchange reactions according to Eq. (3).

$$\lambda_{12} = \frac{\lambda_{11} + \lambda_{22}}{2}. \tag{3}$$

The reorganization energy is the structural energy change imposed by changing the oxidation state. We can thus express $\ln k$ as a function of ΔE^0($\Delta G^0 = -nF\Delta E^0$) according to Eq. (4).

$$\ln k = \ln Z - \frac{\lambda_{12}}{4RT}\left(1 - \frac{nF\Delta E^0}{\lambda_{12}}\right)^2. \tag{4}$$

Consequently, when plotting the logarithm of the rate constant for an electron transfer process against the one-electron reduction potential for the oxidant (assuming we have the same reductant) we would expect a parabolic curve rather than a linear relationship. However, it should be noted that the curvature is strongly dependent on the reorganization energy of the process. For high reorganization energies $\ln k$ appears to be almost linearly related to the one-electron reduction potential in a relatively wide range of potentials while for low reorganization energies the parabolic nature of the relationship becomes obvious even for relatively narrow potential ranges. It should also be noted that plotting $\ln k$ against E^0 or ΔG^0 is only meaningful when the reorganization energy for all oxidants can be assumed to be constant or very low compared to the reorganization energy of the common reductant. Although this relationship was derived for homogeneous reaction systems we can use it to qualitatively assess the behavior of the heterogeneous systems discussed here. Weaver has shown that the rate constant for heterogeneous electron transfer is related to the rate constant for homogeneous electron transfer according to Eq. (5) [14].

$$\frac{k_{het}}{Z_{het}} = \sqrt{\frac{k_{hom}}{Z_{hom}}}, \tag{5}$$

where Z_{het} and Z_{hom} are the collision frequencies for the heterogeneous and the homogeneous system, respectively. Consequently, $\ln k_{het}$ is proportional to $\ln k_{hom}$ thus rationalizing the comparison. The reorganization energies for the self-exchange reactions in the solid metal oxides are not known. However, it is reasonable to assume that high reorganization energy is connected with low electrical conductivity. The conductivity for UO_2 and Fe_3O_4 are $\sigma \approx 10^{-3}\,\Omega^{-1}\,cm^{-1}$ and $\sigma \approx 250\,\Omega^{-1}\,cm^{-1}$, respectively at 300 K [15,16]. Hence, Fe_3O_4 is a considerably better electrical conductor than is UO_2. This implies that the reorganization energy connected with oxidation of UO_2 should be higher than the reorganization energy connected with oxidation of Fe_3O_4 and its Co and Ni analogues. From this reasoning we would expect a plot of $\ln k$ against E^0 for the oxidant to be more parabolic for the Fe_3O_4 system (and its Co and Ni analogues) than for the UO_2 system. Interestingly, this is exactly the trend that we observe experimentally.

Unlike H_2O_2, both oxidants used in this work are anions. Consequently, the kinetics for the reaction between the oxidants and the metal oxides is expected to be significantly affected by the surface charge of the particles. As can be seen in Table 2, the point of zero charge (ZPC) is around 7 for all three metal oxides. At pH below ZPC the surface is positively charged and there should be an electrostatic attraction between the negatively charged oxidants and the metal oxide surfaces. At pH above ZPC there should be an electrostatic repulsion between the oxidants and the metal oxide surfaces due negative surface charge. For this reason we performed all experiments in pure water and at pH 4 (adjusted by adding acetic acid). In Fig. 4 the absorbance of MnO_4^- (in a suspension, unbuffered and at pH 4, containing Fe_2CoO_4) is plotted against reaction time.

As can be seen, oxidation is somewhat faster at the lower pH. The resulting second order rate constants

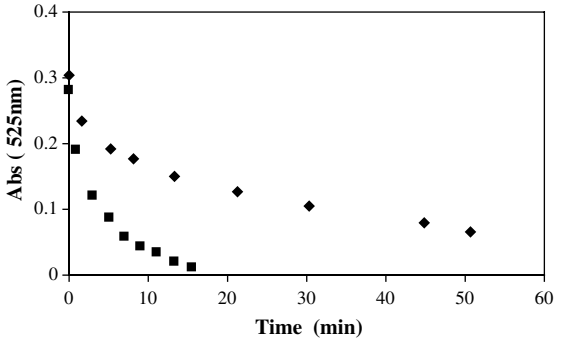

Fig. 4. MnO_4^- absorbance (at 525 nm) as a function of reaction time (with Fe_2CoO_4 at 25 °C) in unbuffered solution (♦) and at pH 4 (▲).

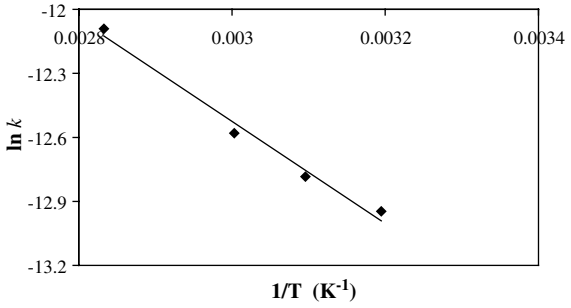

Fig. 5. $\ln k$ for the reaction between MnO_4^- and Fe_3O_4 plotted against $1/T$.

for oxidation of the metal oxides are presented in Table 3.

It is interesting to note that the pH effect on the kinetics of oxidation is most pronounced for the most thermodynamically favored system, i.e. the reaction between $IrCl_6^{2-}$ and Fe_3O_4. This can probably be attributed to the higher charge of the oxidant, which in turn will make the kinetics more sensitive to the charge of the surface. The pH effect on the oxidation of Fe_2NiO_4 is almost insignificant for both oxidants.

The activation energy for the reaction between MnO_4^- and Fe_3O_4 was determined to 20 kJ mol^{-1} (Fig. 5).

For comparison, the activation energy for the reaction between H_2O_2 and Fe_3O_4 was previously determined to 52 kJ mol^{-1} [10]. The significantly lower activation energy for MnO_4^- compared to H_2O_2 is in line with the observed difference in reactivity. The activation energy for the reaction between $IrCl_6^{-2}$ and Fe_3O_4 could not be determined using the present experimental setup as the reaction is too fast even at moderately elevated temperatures.

4. Conclusions

In this study we have shown that the CRUD model compounds Fe_3O_4, Fe_2CoO_4 and Fe_2NiO_4, react with the oxidants $IrCl_6^{2-}$ and MnO_4^- with appreciable rates at room temperatures. The trend in reactivity of the metal oxides with the oxidants is in the line with the previous study employing H_2O_2 as oxidant. The logarithm of the rate constants for the reactions between the metal oxides (Fe_3O_4, Fe_2CoO_4 and Fe_2NiO_4) and the oxidants H_2O_2, $IrCl_6^{2-}$ and MnO_4^-) plotted against the one-electron reduction potentials of the oxidants result in a parabolic curve. This is not the case for oxidation of UO_2 under similar conditions. This discrepancy is explained in terms of differences in the reorganization energy of the metal oxides giving rise to different curvature in accordance with the Marcus theory for electron transfer.

References

[1] Y. Nishino, T. Sawa, K. Ohsumi, H. Itoh, J. Nucl. Sci. Technol. 26 (1989) 1121.
[2] T. Marchl, G.U. Gerger, Water Chem. Reactor Syst. 5 (2) (1989) 13.
[3] R.M. Cornell, U. Schwertmann, The Iron Oxides, VCH Verlagsgesellschaft mbH, Weinheim, 1996 (Chapter 6).
[4] K.J. Gallagher, W. Feitknecht, U. Mannweiler, Nature 217 (1968) 1118.
[5] U. Colombo, G. Fagherazzi, F. Gazzarrini, G. Lanzavecchia, G. Sironi, Nature 219 (1968) 1036.
[6] S.D. Sidhu, R.J. Gilkes, A.M. Posner, J. Inorg. Nucl. Chem. 39 (1977) 1953.
[7] J.P. Jolivet, E. Tronc, J. Colloid Interface Sci. 125 (1988) 688.
[8] L. Zheng-Ya, D.M. Muir, Hydrometallurgy 21 (1988) 9.
[9] E. Ekeroth, M. Jonsson, J. Nucl. Mater. 322 (2003) 242.
[10] M. AbiliNejad, M. Jonsson, J. Nucl. Mater. 334 (2004) 28.
[11] R.A. Marcus, J. Chem. Phys. 24 (1956) 966.
[12] R.A. Marcus, J. Chem. Phys. 26 (1957) 867.
[13] R.A. Marcus, J. Chem. Phys. 43 (1965) 679.
[14] M.J. Weaver, J. Phys. Chem. 84 (1980) 568.
[15] T. Meek, M. Hu, M.J. Haire, Waste Management 2001 Symposium, Tucson, Arizona.
[16] G.A. Samara, Phys. Rev. Lett. 21 (1968) 795.
[17] A.J. Bard, R. Parsons, Standard Potentials in Aqueous Solutions, Marcel Dekker, New York, 1985.
[18] P. Wardman, J. Phys. Chem. Ref. Data 18 (1989) 1637.
[19] R.C. Plaza, J.L. Arias, M. Espin, M.L. Jimenz, J. Colloid Interface Sci. 245 (2002) 86.
[20] M. Kosmulski, J. Colloid Interface Sci. 253 (2002) 77.
[21] J. de Vicente, J.D.G. Durn, A.V. Delgado, Colloids Surf. A 195 (2001) 181.
[22] R.C. Plaza, J. de Vicente, S. Gomez-Lopera, A.V. Delgado, J. Colloid Interface Sci. 242 (2001) 306.
[23] M. Olsson, A.M. Jakobsson, Y. Albinsson, J. Colloid Interface Sci. 256 (2002) 256.